Hindawi Publishing Corporation
International Journal of Antennas and Propagation
Volume 2015, Article ID 878614, 6 pages
http://dx.doi.org/10.1155/2015/878614

Research Article

Radio Capacity Estimation for Millimeter Wave 5G Cellular Networks Using Narrow Beamwidth Antennas at the Base Stations

AlMuthanna Turki Nassar,[1,2] Ahmed Iyanda Sulyman,[2] and Abdulhameed Alsanie[2]

[1] *MRN Planning and Design Department, Mobily (Etihad Etisalat), P.O. Box 9979, Riyadh 11423, Saudi Arabia*
[2] *Department of Electrical Engineering, King Saud University, P.O. Box 800, Riyadh 11421, Saudi Arabia*

Correspondence should be addressed to AlMuthanna Turki Nassar; m.nassar@student.ksu.edu.sa

Received 11 March 2015; Accepted 16 June 2015

Academic Editor: Atsushi Mase

This paper presents radio frequency (RF) capacity estimation for millimeter wave (mm-wave) based fifth-generation (5G) cellular networks using field-level simulations. It is shown that, by reducing antenna beamwidth from 65° to 30°, we can enhance the capacity of mm-wave cellular networks roughly by 3.0 times at a distance of 220 m from the base station (BS). This enhancement is far much higher than the corresponding enhancement of 1.2 times observed for 900 MHz and 2.6 GHz microwave networks at the same distance from the BS. Thus the use of narrow beamwidth transmitting antennas has more pronounced benefits in mm-wave networks. Deployment trials performed on an LTE TDD site operating on 2.6 GHz show that 6-sector site with 27° antenna beamwidth enhances the quality of service (QoS) roughly by 40% and more than doubles the overall BS throughput (while enhancing the per sector throughput 1.1 times on average) compared to a 3-sector site using 65° antenna beamwidth. This agrees well with our capacity simulations. Since mm-wave 5G networks will use arbitrary number of beams, with beamwidth much less than 30°, the capacity enhancement expected in 5G system when using narrow beamwidth antennas would be much more than three times observed in our simulations.

1. Introduction

Radio capacity is of great concern in cellular systems as it directly dictates the achievable data rates. The widespread use of smart phones and tablets and the availability of social network websites, where users can watch, download/share videos, and run many other mobile applications, led to an unprecedented increase in demand for high data rates. Global mobile data traffic reached 1.5 exabytes per month at the end of 2013, with data traffic growth rate of 81 percent in 2013 compared to 2012 [1]. This high demand for cellular data services, especially in large urban markets, puts pressure on operators to keep seeking solutions for realizing higher capacity in their networks. However, with such an explosive growth in data traffic, the existing mobile infrastructures including the 4G systems will be highly congested in the coming few years. This necessitates a disruptive next-generation capacity enhancement solution. Many of the requirements of what is called Beyond 4G (B4G) and 5G to reach multigigabits per second (Gbps) wireless data rates were discussed in [2], where the design of B4G and key technology components were presented. In this work, we examine the capacity of future 5G cellular networks on mm-wave frequency bands.

There is a growing belief that mm-wave frequency bands (30–300 GHz) will play a significant role in B4G and 5G cellular systems because of the huge bandwidths available for cellular services in that band [3, 4]. Recent research works have thus devoted significant efforts to characterizing the mm-wave channels. Path loss and propagation measurements were recently conducted for mm-wave band at various frequencies: 28 GHz, 38 GHz, 60 GHz, and 72 GHz. The work in [5] presented a variety of indoor and outdoor propagation measurements where it was suggested that 28 GHz and 38 GHz bands can in fact be used for cellular systems when

employing steerable directional antennas at the base station (BS) and mobile station (MS). It was also shown in [6] that, with adaptive antenna array beamforming, multi-Gbps data rates can be supported for mm-wave mobile cellular deployments at 28 GHz. Recent studies in [7–9] have also shown that adequate outdoor coverage is possible up to 220 m approximately for mm-wave channels. Such cell size allows the use of low power microcell or picocell base stations with highly directional antennas in conjunction with multibeams techniques for more improvements. The work in [8] presented the achievable radio frequency (RF) coverage and system capacity using mm-wave based cellular systems based on field-level simulations, while the work in [9] develops mm-wave path loss model based on real-world measurements at 28 and 38 GHz. It is shown in [8, 9] that, based on realistic BS radius of 220 m, about four times the number of existing cell sites may be required in the mm-wave based network. In [10], theoretical analysis on the probability of coverage for mm-wave cellular networks was presented, while [11] derives statistical models for key channel parameters including the path loss, number of spatial clusters, angular dispersion, and outage, based on real-world measurements at 28 and 73 GHz in New York City. In this paper, we employ field-level network simulations, typically used by mobile radio operators for cellular planning, to estimate the field-level capacity performance of mm-wave cellular systems at 28 GHz for various antenna beamwidths. We show that narrow beamwidth antennas have more pronounced capacity enhancements in mm-wave networks than in their microwave counterparts.

2. Radio Capacity Expression for Microwave and mm-Wave 5G Networks

An MS located or moving in the coverage area of a serving BS will receive useful signals from the serving BS and interfering signals from other cochannel BS's. The server signal strength varies even when the MS is not moving due to the large-scale fading and small-scale fading factors and also due to the interference received from neighboring cochannel BS's. All these factors determine the strength of the carrier-to-interference ratio (CIR) received by the MS. The CIR is the quotient between the average received modulated carrier power and the average received cochannel interfering power. A large CIR results in high quality of service (QoS), while a small CIR results in low QoS. Radio capacity is dependent on CIR and the available bandwidth (B). The radio capacity for any wireless system can be estimated using the expression

$$C = B\log_2(1 + \mathrm{CIR}), \tag{1}$$

where B denotes the RF channel bandwidth of the system and CIR denotes the carrier-to-interference ratio at various distances from the serving BS [9]. The CIR, in decibels (dB), can be estimated as

$$\begin{aligned}\mathrm{CIR}_{\mathrm{dB}} &= 10\log_{10}(\mathrm{CIR}) \\ &= 10\log_{10}\left(\frac{P_{\mathrm{rec}}(\text{Serving BS})}{\sum P_{\mathrm{rec}}(\text{Interfering BS's})}\right),\end{aligned} \tag{2}$$

where P_{rec} is the received signal strength in watts, either from the serving BS or from the interfering BS's at any distance.

The received signal strength at various distances "d" from the BS, $P_{\mathrm{rec}}(d)$, can be estimated as

$$P_{\mathrm{rec}}(d)\ [\mathrm{dB}] = P_t\ [\mathrm{dB}] - \mathrm{PL}(d)\ [\mathrm{dB}], \tag{3}$$

where P_t [dB] denotes the transmitter (TX) power in dB and PL(d) [dB] is the path loss at distance "d," also in dB. PL(d) [dB] can be estimated using the Hata/COST231-Hata models for microwave networks operating below 2 GHz or using the Stanford University Interim (SUI) model for microwave networks above 2 GHz [9]. For the mm-wave 5G networks, PL(d)[dB] can be estimated using the modified SUI model presented in [9] for the 28 GHz and 38 GHz bands.

2.1. Capacity Estimation for Microwave and mm-Wave Networks Using Narrow Beamwidth BS Antennas. In this section we estimate the radio capacity for mm-wave cellular networks in comparison with its microwave counterparts when reducing the transmitting antenna beamwidth from 65° to 30°. We used trisector BS with TX height of 20 m and EIRP of 63.5 dBm ($Pt = 43$ dBm, TX antenna gain is 20.5 dBi for 30° beamwidth and 17 dBi for 65° beamwidth). A benchmark of $P_{\mathrm{rec}}(d) \geq -75$ dBm outdoor is used at various locations d within the cell for estimating coverage distance. For the mm-wave network, we used this benchmark to arrive at a coverage distance of 220 m, as reported in [5, 9].

Figure 1 shows the RF coverage pattern for a serving BS (site-58) in a 28 GHz mm-wave network for both 65° and 30° antenna beamwidth. The circles around the server BS indicate the tiers of interfering BS's; the inner-most circle denotes the first-neighbor sites, the next circle denotes the second-neighbor sites, and so forth. Figure 2 displays the corresponding RF patterns for the interfering neighbors, with significant received signal strength, on the sector of site-58 in the direction of the arrow shown in the figure. Using the TEMS cell planner [12] and the propagation PL models introduced in [9] for mm-waves at 28 GHz, we measured the received signals from the serving base station (site-58) and the interfering neighbors while moving away from the serving site-58 (upward) in steps of 10 m up to a distance of 220 m. Note that site ID's are on the right-hand side of each site in these figures. Measurement samples are shown in Tables 1 and 2, respectively, for the 65° and 30° antenna beamwidth.

It can be seen from Tables 1 and 2 that deploying narrow beamwidth antennas in mm-wave based 5G networks results in less interference. The received signals from all neighboring sites are less in Table 2 compared to Table 1 especially for the neighboring sites 46, 48, 56, 67, and 69. We can see that for these neighboring sites we did not receive any detectable signal at certain transmitter-receiver (TX-RX) separation distances for the case of 30° beamwidth as was received for the case of 65° beamwidth.

Using the measurement samples in Tables 1 and 2 and applying (1) and (2), we estimate the radio capacity for the mm-wave based 5G cellular network operating on 28 GHz and compare the results with microwave counterparts operating on 900 MHz and 2.6 GHz, using both 65° and 30°

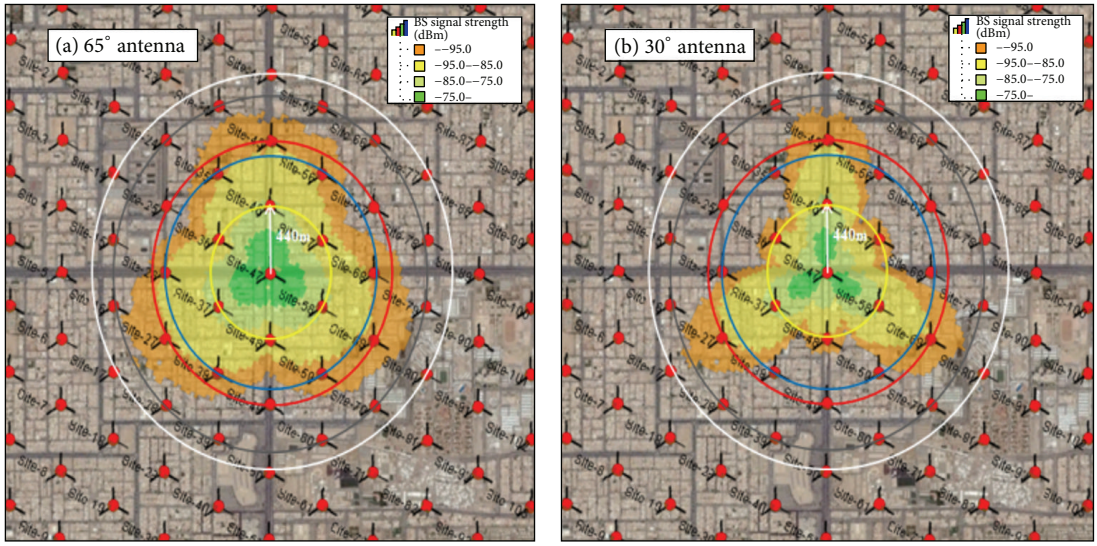

Figure 1: RF coverage of serving trisector BS (site-58) for the sector in the direction of the arrow for $f_c = 28$ GHz and various TX antenna beamwidths: (a) 65°, (b) 30°.

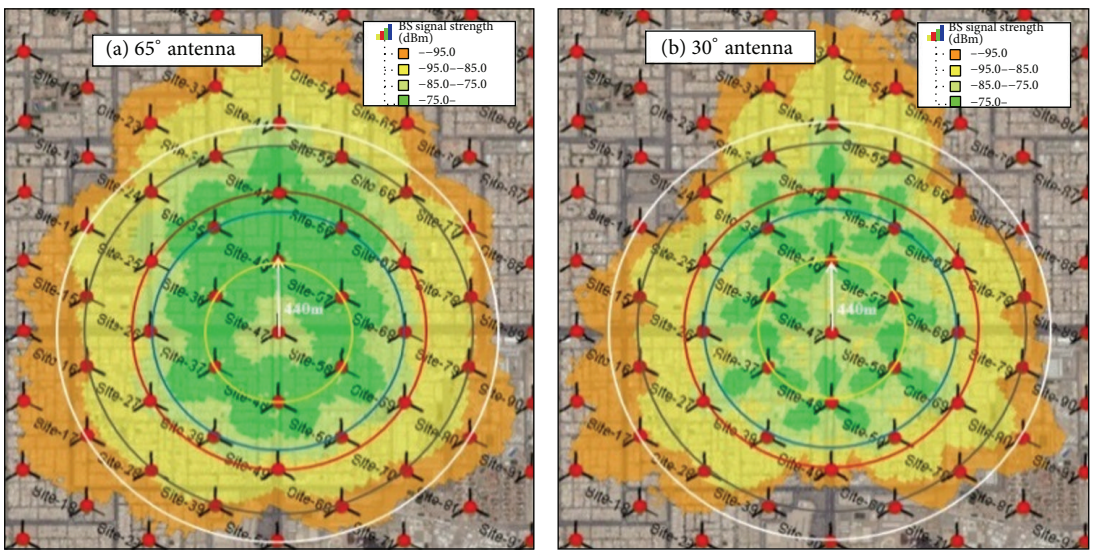

Figure 2: RF coverage of interfering trisector BS's with significant received signal strength on the sector of site-58 in the direction of the arrow for $f_c = 28$ GHz and various TX antenna beamwidths: (a) 65°, (b) 30°.

antenna beamwidths. The resulting capacity enhancements for mm-wave network operating on 28 GHz when reducing antenna beamwidth from 65° to 30° are shown in Figure 3, while counterparts results for microwave networks operating on 900 MHz and 2.6 GHz are shown in Figures 4 and 5, respectively. In general, from Figures 3, 4, and 5, it can be observed that for both the microwave and the mm-wave networks the capacity decreases as the MS moves away from the serving BS, as expected. This is because of the decrease in the CIR as the MS moves away from the serving BS. In such case, the received signal from the serving BS becomes lower due to increasing path loss while the interference becomes higher. Also, it can be observed generally that, for both microwave and mm-wave systems, the capacity is enhanced using narrower beamwidth transmitting antennas compared to the capacity when using the wider beamwidth antennas. The capacity of mm-wave networks however has much more pronounced enhancements using narrower beamwidth antenna than the microwave counterparts; and that is because the interference caused by an mm-wave BS to MS's in the neighboring cells is way less than what is experienced in the microwave-based systems, thanks to the higher PL in the mm-wave bands which limits propagation distance away from the BS and provides better cell-edge coverage than the microwave-based networks [8, 9].

This is an important new insight. For example, the result in Figure 3 suggests that the capacity of 28 GHz mm-wave

Table 1: Carrier and interference measurements for the 28 GHz mm-wave networks using 65° beamwidth TX antennas for the trisector BS's.

Site ID	Server/neighbor	Received signals in dBm at various TX-RX separation distances (m)									
		$d = 20$	$d = 40$	$d = 60$	$d = 80$	$d = 100$	$d = 120$	$d = 150$	$d = 170$	$d = 190$	$d = 220$
58	Server	−63.03	−64.25	−64.88	−65.9	−66.77	−67.52	−68.84	−70.32	−72.58	−75.19
57	1st neighbor	−90.25	−88.41	−87.51	−86.54	−85.56	−83.67	−80.63	−79.9	−78.8	−75.95
68	1st neighbor	−82.61	−82.33	−81.16	−80.2	−79.59	−80.15	−80.83	−81.31	−82.9	−83.34
69	1st neighbor	−90.48	−90.67	−90.67	−90.07	−91.25	−90.59	−89.98	−91.27	−91	−92.23
59	1st neighbor	−84.62	−85.48	−86.37	−87.2	−87.92	−87.93	−91.08	−91.77	−92.44	−92.89
48	1st neighbor	−94.7	−94.44	−94.44	−94.97	−96	−95.65	−95.66	−96.17	−96.17	−95.85
47	1st neighbor	−83.67	−83.76	−82.36	−82.94	−83.21	−83.55	−83.03	−93.48	−93.48	−84.31
46	2nd neighbor	−97.09	−96.42	−96.17	−95.3	−95.3	−94.55	−93.01	−92.82	−92.82	−91.93
67	2nd neighbor	—	—	—	—	—	—	—	—	—	−99.85
56	3rd neighbor	−96.17	−95.2	−95.2	−94.56	−93.51	−91.02	−90.68	−89.9	−89.08	−88.81

Table 2: Carrier and interference measurements for 28 GHz mm-wave networks using 30° beamwidth TX antennas for the trisector BS's.

Site ID	Server/neighbor	Received signals in dBm at various TX-RX separation distances (m)									
		$d = 20$	$d = 40$	$d = 60$	$d = 80$	$d = 100$	$d = 120$	$d = 150$	$d = 170$	$d = 220$	$d = 250$
58	Server	−58.65	−60.38	−60.86	−62.18	−63.2	−64.17	−66.24	−68.86	−73.47	−75.13
57	1st neighbor	−95.8	−94.08	−93.5	−92.17	−90.59	−87.41	−86.46	−83.47	−81.4	−79.15
68	1st neighbor	−83.53	−81.72	−80.72	−81.16	−81.86	−82.98	−84.45	−88.63	−92.65	−96.3
69	1st neighbor	−96.86	−97.7	−97.82	−98.29	−99.79	−99.79	—	—	—	—
59	1st neighbor	−84.77	−85.29	−86.21	−87.08	−87.53	−87.76	−90.66	−91.35	−91.98	−92.62
48	1st neighbor	−99.42	—	—	—	—	—	—	—	—	—
47	1st neighbor	−84.28	−82.78	−83.22	−84.33	−85.53	−87.25	−89.01	−91.53	−96.52	−98.94
46	2nd neighbor	—	—	—	—	−98.77	−97.71	−95.9	−94.79	−90.26	−90.26
67	2nd neighbor	—	—	—	—	—	—	—	—	—	—
56	3rd neighbor	—	—	—	—	−99.25	−96.74	−94.99	−94.01	−91.6	−90.39

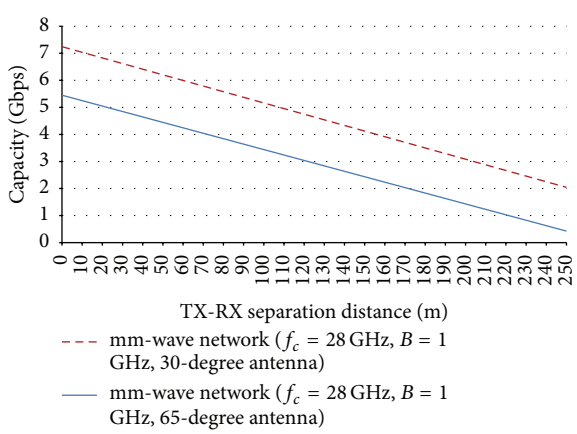

Figure 3: Capacity trend in Gbps for 28 GHz mm-wave networks using 65° and 30° transmitting antenna beamwidths.

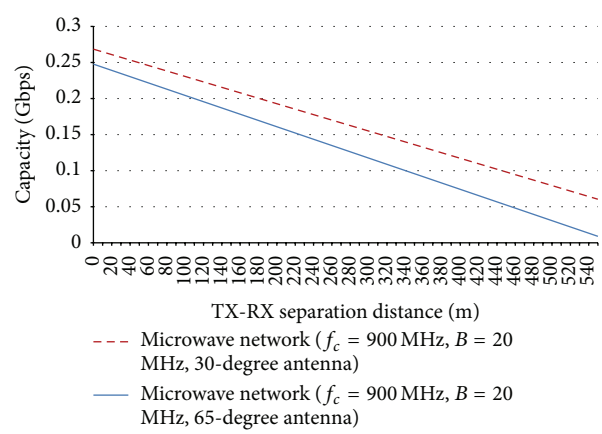

Figure 4: Capacity trend in Gbps for 900 MHz microwave networks using 65° and 30° transmitting antenna beamwidths.

cellular networks is roughly enhanced by 3.0 times at a distance of 220 m from the BS, when reducing TX antenna beamwidth from 65° to 30°. This enhancement is far much higher than the corresponding enhancement of 1.2 times observed in Figures 4 and 5 for the 900 MHz and 2.6 GHz microwave networks at the same distance from the BS. This result means that a capacity enhancement of 300% at cell-edge is possible in a 28 GHz mm-wave network by just reducing antenna beamwidth from 65° to 30°. Mm-wave 5G networks will employ multibeam RF signals, with arbitrary beamwidth much less than 30°. Therefore it is expected that this narrowing of antenna beamwidth transmission strategy alone can scale up capacity significantly and help realize gigabits per second data rates everywhere in the 5G network, including cell edges. For indoor coverage, cell enhancers and in-building RF infrastructures may be needed to insure providing acceptable received power levels inside buildings with satisfying in-building data rates.

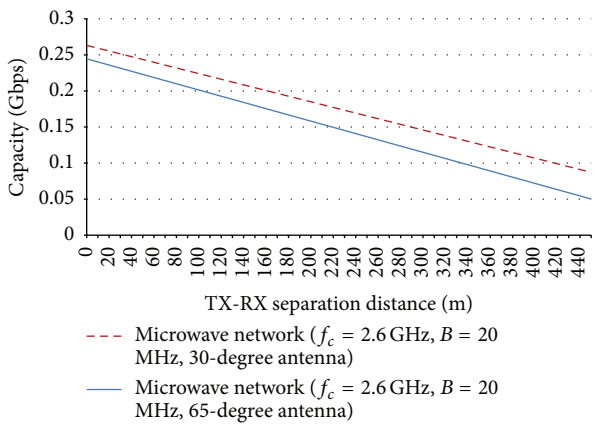

Figure 5: Capacity trend in Gbps for 2.6 GHz microwave networks using 65° and 30° transmitting antenna beamwidths.

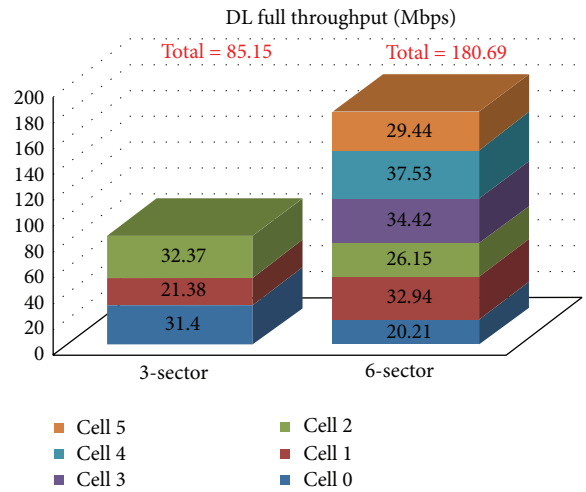

Figure 6: The cell full downlink throughput in Mbps before and after the 6-sector integration.

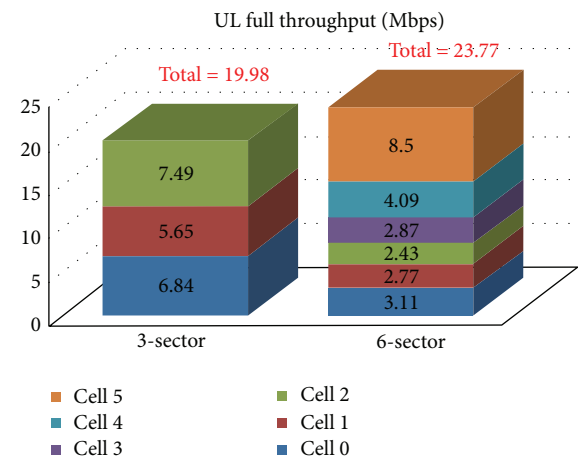

Figure 7: The cell full uplink throughput in Mbps before and after the 6-sector integration.

3. Field Deployment Trials for Narrow Beamwidth Antennas Using 4G LTE

Next we present results from field deployment trials on the capacity enhancements achieved when migrating from 65° to 27° antenna beamwidth in a 4G LTE network using multibeam transmitting antennas. This trial is performed on an LTE TDD site which operates at 2.6 GHz band. The site is originally a 3-sector site with antenna height of 30 m. It was then converted to a 6-sector site during the trials using the following configurations. Each 4Tx-4Rx sector is split into two 2Tx-2Rx sectors. Therefore, for a 3-sector 4Tx-4Rx site, this solution will result in a 6-sector 2Tx-2Rx site using 4-port multibeam transmitting antenna, with each of 2 ports used for one 2Tx-2Rx sector. The new 4-port multibeam antenna has a gain of 20.1 dBi, horizontal beamwidth of 27°, and vertical beamwidth of 4.8°, while the old 4-port antenna has a gain of 17.3 dBi and horizontal and vertical beamwidths of 65° and 6.5°, respectively. Large numbers of users are on this LTE test site before the trial since it serves a dense urban area in Dammam city, Saudi Arabia.

The BS full (overall) throughput is the throughput when all the radio blocks (RB) at the BS sites are loaded up. The RB is the basic unit of radio resource in LTE. One RB occupies 180 KHz portion of the 20 MHz carrier signal bandwidth used. The BS full throughput reports are as shown in Figures 6 and 7, respectively, for the downlink (DL) and uplink (UL). As shown in these figures, significant enhancements in the UL and DL full throughput are observed using 6 sectors. The DL BS full throughput is improved by 112%, while the UL BS full throughput is improved by 19%. The DL per sector throughput corresponds to our capacity simulation above since we consider only one sector (transmission from the BS sector to the users), in the capacity simulations. The average per sector DL throughput is enhanced only 1.1 times using 6-sector site compared to the 3-sector counterpart for the 2.6 GHz microwave network. This agrees closely with the 1.2 capacity enhancements reported in our simulations. Although deployment trails for mm-wave network are currently not possible, the close agreement between the 2.6 GHz microwave network simulation and the field trials results is another way to validate our simulation results obtained for the mm-wave case.

For the user throughput, significant enhancements are observed after the 6-sector integration as shown in Figure 8. DL average user throughput is more than doubled in some cases, while the UL average user throughput improved only slightly. This is due to the fact that directional antennas are currently not implemented on the user mobile devices participating in this trial. Thus the beamwidth changes at the BS will only affect DL transmission to users appreciably. If narrow beamwidth antennas are introduced at the BS and mobiles, then both UL and DL enhancements would be observed. This case cannot be implemented in the deployment trials yet.

The service drop rate is the rate at which connections are lost during the service. This is a measure of the QoS provided by the operator. The service drop rate significantly improved after the integration of 6 sectors as shown in Figure 9. It is enhanced by 42% on average compared to the 3-sector scenario.

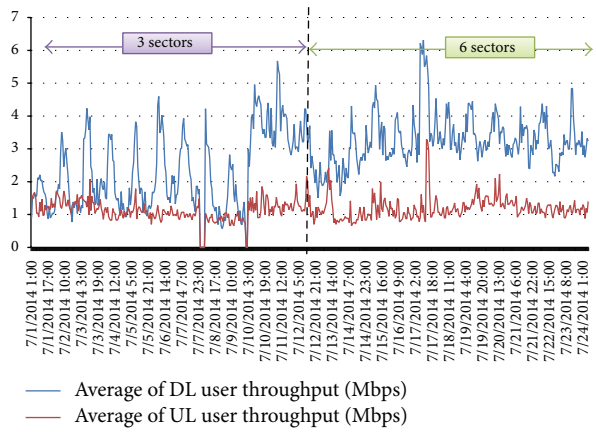

Figure 8: The uplink and downlink user throughput in Mbps before and after the 6-sector integration.

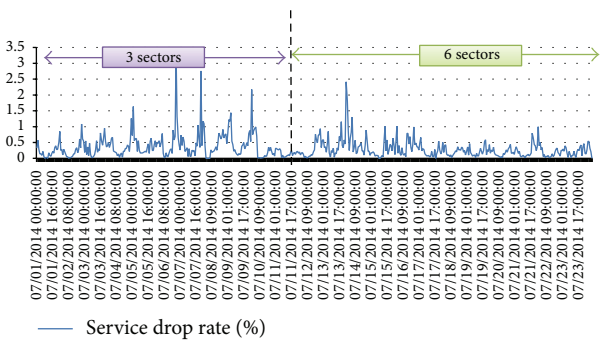

Figure 9: The site service drop rate before and after the 6-sector integration.

The site trial results presented above corroborate the trends observed in our simulations; namely, capacity and QoS can be significantly enhanced migrating from 65° antenna beamwidth to narrower beamwidths. 5G networks will employ narrow antenna beamwidth similar to the ones used in this trial; therefore we expect this solution to enhance the capacity and QoS in 5G networks significantly.

4. Conclusions

This paper presents radio capacity estimation for mm-wave based 5G cellular networks using field-level simulations. It is shown that the capacity of microwave and mm-wave networks can be enhanced using narrow beamwidth transmitting antennas. More pronounced capacity enhancements, roughly more than double, are observed for the mm-wave networks compared to the microwave counterpart at a TX-RX separation distance of 220 m, when moving from 65° to 30° TX antennas. Thus it is concluded that narrow beamwidth solution can help 5G systems to realize gigabits per second data rates everywhere in the network including the cell edges. Deployment trials performed on an LTE TDD site corroborate our findings in the simulation studies. The trial results show that BS overall DL throughput will be doubled and the service drop rate will be enhanced roughly by 40%.

Conflict of Interests

The authors declare that there is no conflict of interests regarding the publication of this paper.

Acknowledgment

This work was funded by the National Plan for Science, Technology and Innovation (MAARIFAH), King Abdulaziz City for Science and Technology, Saudi Arabia, Award Number 11ELE1854-02.

References

[1] Cisco, "Cisco visual networking index: global mobile data traffic forecast update, 2013–2018," White Paper, 2015, https://www.cisco.com/c/en/us/solutions/collateral/service-provider/visual-networking-index-vni/white_paper_c11-520862.pdf.

[2] P. E. Mogensen, K. Pajukoski, B. Raaf et al., "B4G local area: high level requirements and system design," in *Proceedings of the IEEE Globecom Workshops*, pp. 613–617, December 2012.

[3] F. Boccardi, R. W. Heath Jr., A. Lozano, T. L. Marzetta, and P. Popovski, "Five disruptive technology directions for 5G," *IEEE Communications Magazine*, vol. 52, no. 2, pp. 74–80, 2014.

[4] Z. Pi and F. Khan, "An introduction to millimeter-wave mobile broadband systems," *IEEE Communications Magazine*, vol. 49, no. 6, pp. 101–107, 2011.

[5] T. S. Rappaport, S. Sun, R. Mayzus et al., "Millimeter wave mobile communications for 5G cellular: it will work!," *IEEE Access*, vol. 1, pp. 335–349, 2013.

[6] S. Rajagopal, S. Abu-Surra, Z. Pi, and F. Khan, "Antenna array design for multi-Gbps mmwave mobile broadband communication," in *Proceedings of the IEEE Global Telecommunications Conference (GLOBECOM '11)*, pp. 1–6, Houston, Tex, USA, December 2011.

[7] S. Rangan, T. S. Rappaport, and E. Erkip, "Millimeter-wave cellular wireless networks: potentials and challenges," *Proceedings of the IEEE*, vol. 102, no. 3, pp. 366–385, 2014.

[8] A. T. Nassar, A. I. Sulyman, and A. Alsanie, "Achievable RF coverage and system capacity using millimeter wave cellular technologies in 5G networks," in *Proceedings of the 27th IEEE Canadian Conference on Electrical and Computer Engineering (CCECE '14)*, pp. 1–6, IEEE, Toronto, Canada, May 2014.

[9] A. I. Sulyman, A. T. Nassar, M. K. Samimi, G. R. MacCartney Jr., T. S. Rappaport, and A. Alsanie, "Radio propagation path loss models for 5G cellular networks in the 28 and 38 GHz millimeter wave bands," *IEEE Communications Magazine*, vol. 52, no. 9, pp. 78–86, 2014.

[10] S. Akoum, O. El Ayach, and R. W. Heath, "Coverage and capacity in mmWave cellular systems," in *Proceedings of the Conference Record of the Forty Sixth Asilomar Conference on Signals, Systems and Computers (ASILOMAR '12)*, pp. 688–692, IEEE, Pacific Grove, Calif, USA, November 2012.

[11] M. R. Akdeniz, Y. Liu, M. K. Samimi et al., "Millimeter wave channel modeling and cellular capacity evaluation," *IEEE Journal on Selected Areas in Communications*, vol. 32, no. 6, pp. 1164–1179, 2014.

[12] TEMS CellPlanner (TCP) tool, 2014, http://www.mentum.com.